

Pion Double Charge Exchange at 50 MeV on ^{14}C

I. Navon,^(a) M. J. Leitch,^(b) D. A. Bryman,^(a) T. Numao,^(a) and P. Schlatter^(a)
Department of Physics, University of Victoria, Victoria, British Columbia V8W2Y2, Canada

and

G. Azuelos^(a) and R. Poutissou^(a)
Département de Physique, Université de Montréal, Montréal, Quebec H3C 3J7, Canada

and

R. A. Burnham,^(a) M. Hasinoff,^(a) and J. M. Poutissou^(a)
Department of Physics, University of British Columbia, Vancouver, British Columbia V6T 2A6, Canada

and

J. A. Macdonald and J. E. Spuller
Tri-University Meson Facility, Vancouver, British Columbia V6T 2A3, Canada

and

C. K. Hargrove and H. Mes
National Research Council of Canada, Ottawa, Ontario K1A 0R6, Canada

and

M. Blecher and K. Gotow
Virginia Polytechnic Institute and State University, Blacksburg, Virginia 24061

and

M. Moinester
Department of Physics, Tel-Aviv University, Ramat-Aviv, Israel

and

H. Baer
Los Alamos National Laboratory, Los Alamos, New Mexico 87545
 (Received 18 October 1983)

The first measurement of pion double charge exchange at low energy is reported. The reaction $^{14}\text{C}(\pi^+, \pi^-)^{14}\text{O}$ was measured at an incident pion energy of 50 MeV. Differential cross sections of the double analog transition are given in the angular range 50° – 120° . Strong nonanalog transitions were also observed.

PACS numbers: 25.80.Fm

Pion double charge exchange (DCX) is one of the most interesting pion-nucleus reactions. Since at least two nucleons must take part in the interaction, it is regarded as a sensitive probe for nucleon-nucleon correlations. The reaction depends on the nuclear isospin structure, and therefore can be used to study the matter distribution. Calculations of low-energy DCX¹ are still few, and the proper form of the potential is not known. Until 1977, the experimental data were sparse and of poor quality, mainly because of the low cross sections ($\sim 1 \mu\text{b}/\text{sr}$) that characterize this reaction. In recent years new experimental results in the (3, 3) resonance region and above were published (see partial list Refs. 2–6, and a compilation in Nann *et al.*⁴), but there have been

no measurements below 80 MeV.

In this Letter we report on the first measurement of DCX at low energy, performed with the time projection chamber (TPC) on the M9 channel at TRIUMF. The TPC (see Fig. 1) is a hexagonal-shaped large-volume drift chamber situated in uniform parallel electric and magnetic fields, from which three-dimensional tracking information is obtained. The resulting track reconstruction has a precision of 0.2–0.5 mm in the x - y plane and 0.3 cm along the z axis (beam direction). The capability of charge identification by a curvature measurement combined with the large solid angle makes the TPC suitable for measuring the small cross sections of the DCX reaction. More information about the TPC construction and op-

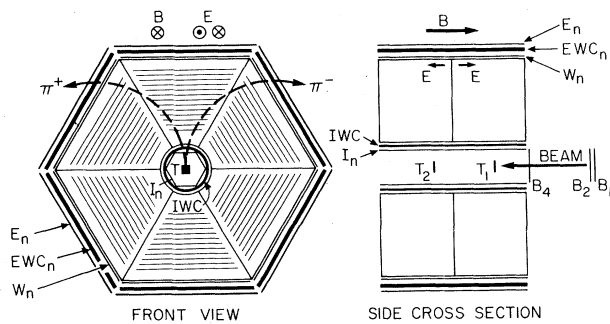


FIG. 1. The TPC front and side cross sections. The targets (T) and the beam (B1, B2, B4) and triggering counters (I_n , IWC, W_n , EWC $_n$, E_n) are shown, as well as the direction of the magnetic (B) and electric (E) fields. The twelve straight lines inside every sector of the TPC are the anode wires; the cathode pads along the anodes are not shown. The two dashed semi-circles coming from the center are examples of X - Y projections of tracks of negative and positive particles.

eration can be found in Hargrove *et al.*⁷

^{14}C was chosen as a target because as a light $T=1$ nucleus, its DCX cross section to the double isobaric analog state (DIAS) was expected to be relatively large, and the separation of the DIAS in ^{14}O (the ground state) from the other nuclear levels is more than 5 MeV. The ^{14}C powder (82% enriched) was enclosed in two thin copper boxes ($50 \times 50 \times 6$ mm³), each containing 0.187 g/cm² of carbon and having windows of 0.046 g/cm² of copper. The two targets were used simultaneously, perpendicular to the beam, one 21 cm upstream from the TPC midplane, and the other 9 cm downstream from it. This arrangement allowed a large angular range, and still maintained enough angular overlap to check on possible systematic effects. The pion beam energy between the two targets was 50 MeV with a flux of 10^6 π^+ /s, with a momentum bite of $\Delta P/P = 2.3\%$, produced by a 30- μA beam of 500-MeV protons striking a 1-cm Cu production target. The pion beam was monitored by three plastic scintillators of thicknesses 1.6, 1.6, and 3.2 mm, 40–70 cm upstream from the target. Electron and muon contaminations in the beam (each approximately 11%) were identified by time-of-flight measurements between the beam scintillators and the rf signal of the cyclotron.

The triggering system (see Fig. 1) included the beam counters, a hexagonal set of six scintillators (I counters), a cylindrical wire chamber (IWC) inside the TPC, and a hexagonal three-layer sandwich outside the TPC composed of

scintillators (W and E counters) and six wire chambers (EWC). The trigger logic required the beam counters to be in coincidence with two inner detectors (I and IWC) and two out of the three outer detector sets (W, EWC, E). The sectorized structure of the system made possible charge preselection by the requirement that the outer counter that fired be one sector clockwise (or counterclockwise) from the inner counter sector. In this way, we could reject elastic scattering at the trigger level, bringing the trigger rate down to an acceptable level of $\leq 5/\text{s}$.

The analysis of the data was straightforward. The false triggers (mostly scattering in the I scintillators) were eliminated by the requirement that the track must come from the target region and have the correct polarity (curvature). The only serious source of background was high-energy electrons produced in the target by conversion of energetic photons. These photons could be produced by pion single charge exchange followed by asymmetric decay of the π^0 . Negatively charged high-energy electrons (momentum range 90–130 MeV/c) outnumbered the DCX pions by a ratio of about four to one, and so strict energy-loss cuts on the I scintillator, W scintillator, and the TPC signals were used to identify electrons and pions. The same cuts applied to elastic scattering runs used for normalization indicated an efficiency loss of about 25%.

Since the Q value for the DCX reaction on ^{14}C is -3.97 MeV, we compared our DCX data to elastic scattering of negative pions at 45 MeV (Fig. 2). The double analog peak is at 46 MeV, and so the elastic scattering was shifted up by 1 MeV to match it in Fig. 2. The nonanalog DCX transitions are seen to be of comparable strength to the DIAS. The nonanalog part is probably a sum of several unresolved levels, and it is truncated at 31 MeV by the experimental cutoff (determined by the minimum momentum required for a particle to reach the external trigger counters). The angle-integrated data shown in Fig. 2 were corrected for the energy difference between the targets (0.6 MeV), for kinematic shift, and for average energy losses in the target, the TPC inner frame, and the I counters. The observed resolution (7.5 MeV, full width at half maximum) is a result of the beam momentum spread, actual energy losses in the target, energy straggling in the I scintillators and the inner TPC frame, and the intrinsic track reconstruction accuracy. In most angular bins the resolution was about 5.5 MeV with the exception of the 90° region, where

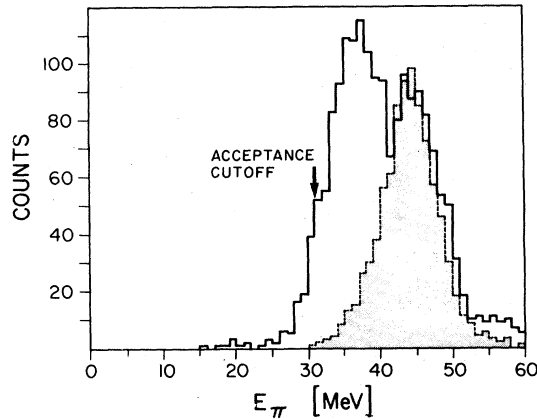


FIG. 2. Angle-integrated spectra of π^- scattering at 45 MeV (dashed line) and (π^+, π^-) at 50 MeV (solid line). The scattering spectrum was normalized to the DIAS and shifted by 1 MeV to match the DIAS energy of 46 MeV.

the energy losses in the targets became dominant.

To determine the number of counts in the DIAS peak at each angular bin and for each target, we integrated the counts in the energy region 41–52 MeV (see Fig. 2). This method was judged to be more reliable than peak fitting because the number of counts in some of the angular bins was too low to define a line shape. Our method implicitly assumes that since the observed strengths of the DIAS and the nonanalog transitions are similar, the contribution of the nonanalog part above 41 MeV is roughly equal to that of the DIAS below 41 MeV. This assumption is not rigorously valid in every angular bin, and the associated errors were included in the error evaluation. To obtain the angular distribution a normalization for the TPC acceptance as a function of the scattering

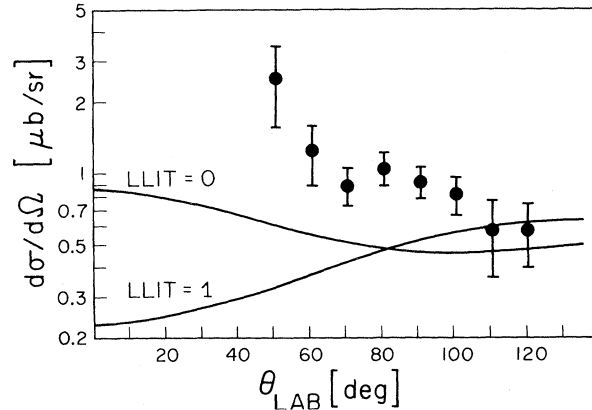


FIG. 3. Angular distribution of $^{14}\text{C}(\pi^+, \pi^-)$ at 50 MeV. The errors are the full angle-dependent errors (including the acceptance errors). The two solid lines are results of theoretical calculations with (LLIT=1) and without (LLIT=0) isotensor term in the potential (Ref. 1).

angle was obtained by means of elastic-scattering runs of π^+ and π^- on ^{14}C and ^{12}C at 50, 45, 40, and 36 MeV. The existing measurements⁸ of positive- and negative-pion elastic scattering on ^{14}C at 50 MeV were used to extract the TPC acceptance for each target separately. Existing elastic-scattering data on ^{12}C ^{9–12} were used to check this normalization and to establish the momentum (energy) acceptance. The uncertainties in the derived acceptance function are a combination of the uncertainties in the normalization data and the statistical uncertainty in our elastic scattering runs.

To evaluate the background, we noted that the DCX reaction on ^{12}C is completely suppressed by the negative Q value of -31.05 MeV. Therefore the ^{12}C content in the ^{14}C target did not contribute

TABLE I. DCX differential cross sections ($\mu\text{b}/\text{sr}$). The errors in columns 2 and 3 are statistical only. The final errors, including those due to the normalization, are given in the last column.

Laboratory angle (deg)	Target 1 (Statistical error only)	Target 2	Weighted average (Total error)
50	2.5 ± 0.3	...	2.5 ± 0.9
60	1.22 ± 0.12	...	1.22 ± 0.33
70	0.91 ± 0.12	0.85 ± 0.11	0.88 ± 0.15
80	1.01 ± 0.11	1.10 ± 0.12	1.05 ± 0.16
90	0.97 ± 0.09	0.86 ± 0.11	0.92 ± 0.13
100	0.81 ± 0.11	0.83 ± 0.14	0.82 ± 0.15
110	...	0.57 ± 0.10	0.57 ± 0.20
120	...	0.57 ± 0.10	0.57 ± 0.16

to the DCX. A separate DCX run on a ^{12}C target thus gave only electron background. The background from those misidentified electrons and from DCX in the Cu box was evaluated with use of the DCX runs on ^{12}C and on empty Cu boxes. Each of these runs gave two counts in the energy region 41-52 MeV, with a normalization factor (integrated beam times target thickness) of 12, so that the background under the DIAS peak was evaluated as 48 ± 24 out of 759 counts (about 7%). Since the background runs gave too few counts to make an angular distribution, an overall subtraction of 7% was done for all the angular bins. The results for both targets and the final weighted averages are listed in Table I. The latter are also displayed in Fig. 3. An overall normalization uncertainty of 18% has been introduced.

This first measurement of DCX at low energy could serve to put a constraint on theoretical calculations. Some prominent features are apparent in the present results: The shape of the angular distribution has some resemblance to that of elastic scattering but the minimum at 70° is much shallower. The angular distribution seems to rise at forward angles, unlike that for single charge exchange¹² which has a minimum at 0° . The nonanalog transitions are as strong as the DIAS transition—the same surprising result was first observed at the resonance energy.⁴ Optical-model calculations using a modified version of the code PIESEX¹ were done by Siciliano. The parameters chosen gave good agreement with 50-MeV single charge exchange on ^{15}N , and 50-MeV

elastic scattering on ^{16}O .¹³ Shown with the experimental data in Fig. 3 are the results of the calculations with and without the isotensor Lorentz-Lorenz term. They have the right magnitude, but the shape has only a modest resemblance to the data. A better theoretical understanding and more data are desirable.

^(a)Mailing address: TRIUMF, 4004 Wesbrook Mall, Vancouver, B.C. V6T 2A3, Canada.

^(b)Present address: Los Alamos National Laboratory, Los Alamos, N. Mex. 87545.

¹E. R. Siciliano, private communication; M. B. Johnson and E. R. Siciliano, Phys. Rev. C **27**, 1647 (1983).

²R. L. Burman *et al.*, Phys. Rev. C **17**, 1774 (1978).

³S. J. Greene *et al.*, Phys. Rev. C **25**, 924, 927 (1982); G. R. Burleson *et al.*, Phys. Rev. C **22**, 1180 (1980).

⁴K. K. Seth *et al.*, Phys. Rev. Lett. **43**, 1574 (1979), and **45**, 147(E) (1980); K. K. Seth, in Los Alamos Scientific Laboratory Report No. LA-7829-C, p. 201, Proceedings of the LAMPF Workshop on Pion Single Charge Exchange (unpublished); H. Nann *et al.*, Phys. Lett. **96B**, 261 (1980).

⁵R. E. Mischke *et al.*, Phys. Rev. Lett. **44**, 1197 (1980).

⁶J. Davis *et al.*, Phys. Rev. C **20**, 1946 (1979).

⁷C. K. Hargrove *et al.*, to be published.

⁸M. Blecher, private communication.

⁹M. Blecher *et al.*, Phys. Rev. C **20**, 1884 (1979).

¹⁰B. M. Freedom *et al.*, Phys. Rev. C **23**, 1134 (1981).

¹¹G. H. Dow, M. Sc. thesis, New Mexico State University, 1981 (unpublished).

¹²J. Alster and J. Warszawski, Phys. Rep. **52**, 87 (1979).

¹³M. D. Cooper *et al.*, to be published.